Periodic *GW* calculations in the Gaussian and plane waves scheme

Jan Wilhelm[*] and Jürg Hutter

Department of Chemistry, University of Zurich, Winterthurerstrasse 190, CH-8057 Zurich, Switzerland

(Dated: June 7, 2017)

We present a correction scheme for periodic Γ-only *GW* calculations in a Gaussian basis. For four benchmark systems, the dependence of the corrected *GW* quasiparticle levels on the cell size is reduced by a factor of three to ten compared to *GW* calculations without correction. The correction scheme comes along with negligible computational cost and enables *GW* calculations for supercells containing hundreds of atoms with Gaussian basis functions.

I. INTRODUCTION

The accurate prediction of photoelectron spectroscopy is still a major computational challenge in many fields of physics, chemistry, and materials science.[1] For medium and large systems, the most used method is Kohn-Sham (KS) density functional theory.[2] As it is well-known, using KS-DFT eigenvalues for computational spectroscopy has a serious fundamental and practical limitation: Depending on the parametrization of the exchange-correlation functional, the KS-DFT eigenvalues can shift substantially.

The *GW* approximation[3] promises better accuracy for the calculation of quasiparticle energy levels. Besides the search for more accurate *GW* flavours[4–7], the main challenges of *GW* is related to the high computational cost and numerical issues. Therefore, it is not surprising that it took more than twenty years between proposing the *GW* method by Hedin[3] and the first application to real materials by Hybertsen and Louie[8].

Significant progress has been made in reducing the computational cost of *GW* in recent years: Plane-wave *GW* implementations commonly suffer from requiring many virtual states and the inversion of large dielectric matrices. Here, the comination of without-virtual-states techniques[9–11] with a low-rank approximation of the dielectric matrix[10,12–15] can improve the computational efficiency enabling large-scale applications[16–18]. Another approach is to reformulate *GW* in a Gaussian basis which can significantly reduce the dimensionality of the involved matrices[19–29]. *GW* in a Gaussian basis can be applied to molecules without difficulty[30–40] in contrast to plane-waves implementations where several technical issues have to be addressed[10,41,42]. Large-scale *GW* calculations also have been reported using stochastic orbitals[43,44].

Another issue of periodic *GW* is the necessity for a correction due to the spurious self-interaction between periodic images of quasiparticle wavefunctions. This self-interaction results in a slow $1/L$ convergence of the *GW* quasiparticle levels with the cell length L. In case of Brillouin zone sampling, the $1/L$ convergence translates to a $N_{\mathbf{k}}^{-1/3}$ convergence with the number of *k*-points.[45] A similar slow convergence as in *GW* has been found for coupled cluster[46,47] and Hartree-Fock exchange in the condensed phase. For the latter, various corrections exist that aim to accelerate the Brillouin zone convergence, including auxiliary function techniques[48] and real-space truncation of the Coulomb interaction[49–51].

For plane-waves implementations of *GW*, several correction schemes have been proposed to correct for this slow convergence: Analytic integration of the divergence at the Γ-point[8,52,53] which is suitable in case of dense *k*-point sampling, the Γ-offset method[54–56], or Brillouin zone integration using analytical limits at the Γ-point[10,41,45,57,58]. In the pioneering implementation of periodic *GW* with Gaussians by Rohlfing *et al.*[24,25], which is so far the only implementation of periodic *GW* in a Gaussian basis to the best of our knowledge, dense *k*-point sampling is used while the periodic correction has been computed in a plane-waves basis.

In this work, we propose a correction scheme for periodic Γ-only *GW* calculations in a Gaussian basis. In Sec. II, we derive our correction scheme in detail. We show benchmark calculations on four materials in Sec. III.

II. DERIVATION OF THE CORRECTION TO THE PERIODIC *GW* SELF-ENERGY IN A GAUSSIAN BASIS

In this section, we derive a correction for periodic *GW* calculations that accelerates the slow $1/L$ convergence of *GW* quasiparticle energies with the cell length L. In Sec. II A, we start with a brief review of periodic *GW* calculations in a plane-waves basis. Then, the derivation is tailored to the use of Gaussian basis functions and the resolution of the identity with the overlap metric (Sec. II B). To apply the correction schemes from plane-waves *GW*, we express the screened Coulomb interaction, the dielectric matrix and the polarizability as square matrices in the resolution-of-the-identity (RI) basis, which corresponds to a plane-waves basis in plane-waves *GW* (Sec. II C). For the correction scheme, we add the $\mathbf{G} = 0$ function to the RI basis, see Sec. II D. The *k*-dependence of the polarizability, the dielectric function and the screened Coulomb interaction is needed for the correction and given in Sec. II E. Using the *k*-dependence of the screened Coulomb interaction and Brillouin zone sampling, we integrate the singularity in the self-energy, see Sec. II F. Finally, we give the algorithm for periodic *GW* calculations in a Gaussian basis in Sec. II G.

A. Periodic *GW* calculations in a plane-waves basis

In this section, we summarize periodic *GW* calculations in a plane-waves basis with a focus on the divergence of the screened Coulomb interaction at the Γ-point. The equations are taken from Refs. 52, 58 and 59.

The equation for computing the G_0W_0 bandstructure $\varepsilon_{n\mathbf{k}}^{G_0W_0}$ reads[52,58]

$$\varepsilon_{n\mathbf{k}}^{G_0W_0} = \varepsilon_{n\mathbf{k}}^{\mathrm{DFT}} + Z_{n\mathbf{k}}\mathrm{Re}\,\langle n\mathbf{k}|\Sigma^{\mathrm{c}}(\varepsilon_{n\mathbf{k}}^{\mathrm{DFT}}) + \Sigma^{\mathrm{x}} - V_{\mathrm{DFT}}^{\mathrm{xc}}|n\mathbf{k}\rangle \quad (1)$$

where we focus on the correlation part $\Sigma_{n\mathbf{k}}^{\mathrm{c}}$ of the self-energy in this work. On the imaginary frequency axis and using a plane-waves basis, it can be computed as

$$\Sigma_{n\mathbf{k}}^{\mathrm{c}}(i\omega) = -\frac{1}{2\pi}\frac{1}{\Omega}\sum_{\mathbf{q}}^{\mathrm{1.\,BZ}}\sum_{m}^{\mathrm{all}}\int_{-\infty}^{\infty}d\omega'\frac{1}{i(\omega-\omega')+\varepsilon_{\mathrm{F}}-\varepsilon_{m\mathbf{k}-\mathbf{q}}}$$
$$\times\sum_{\mathbf{G}\mathbf{G}'}A_{\mathbf{G},\mathbf{q}}^{n\mathbf{k},m\mathbf{k}-\mathbf{q}}W_{\mathbf{G}\mathbf{G}'}^{\mathrm{c}}(i\omega',\mathbf{q})\left(A_{\mathbf{G}',\mathbf{q}}^{n\mathbf{k},m\mathbf{k}-\mathbf{q}}\right)^{*} \quad (2)$$

where $\Omega = \Omega_{\mathrm{cell}}/N_{\mathbf{k}}$ and $A_{\mathbf{G},\mathbf{q}}^{n\mathbf{k},m\mathbf{k}-\mathbf{q}}$ is given by

$$A_{\mathbf{G},\mathbf{q}}^{n\mathbf{k},m\mathbf{k}-\mathbf{q}} = \langle n\mathbf{k}|e^{i(\mathbf{q}+\mathbf{G})\mathbf{r}}|m\mathbf{k}-\mathbf{q}\rangle\,. \quad (3)$$

The correlation part of the screened Coulomb interaction reads

$$W_{\mathbf{G}\mathbf{G}'}^{\mathrm{c}}(i\omega,\mathbf{q}) = \frac{\sqrt{4\pi}}{|\mathbf{q}+\mathbf{G}|}\left(\epsilon_{\mathbf{G}\mathbf{G}'}^{-1}(i\omega,\mathbf{q})-\delta_{\mathbf{G}\mathbf{G}'}\right)\frac{\sqrt{4\pi}}{|\mathbf{q}+\mathbf{G}'|}\,, \quad (4)$$

and the symmetric dielectric function is given by

$$\epsilon_{\mathbf{G}\mathbf{G}'}(i\omega,\mathbf{q}) = \delta_{\mathbf{G}\mathbf{G}'} - \frac{\sqrt{4\pi}}{|\mathbf{q}+\mathbf{G}|}\chi_{\mathbf{G}\mathbf{G}'}^{0}(i\omega,\mathbf{q})\frac{\sqrt{4\pi}}{|\mathbf{q}+\mathbf{G}'|}\,, \quad (5)$$

where $\chi_{\mathbf{G}\mathbf{G}'}^{0}(i\omega,\mathbf{q})$ is the independent particle polarizability,

$$\chi_{\mathbf{G}\mathbf{G}'}^{0}(i\omega,\mathbf{q}) = \frac{1}{\Omega}\sum_{\mathbf{k}ia}^{\mathrm{occ,virt}}A_{\mathbf{G},\mathbf{q}}^{i\mathbf{k},a\mathbf{k}-\mathbf{q}}\frac{2(\varepsilon_{i\mathbf{k}}-\varepsilon_{a\mathbf{k}-\mathbf{q}})}{\omega^2+(\varepsilon_{i\mathbf{k}}-\varepsilon_{a\mathbf{k}-\mathbf{q}})^2}\left(A_{\mathbf{G}',\mathbf{q}}^{i\mathbf{k},a\mathbf{k}-\mathbf{q}}\right)^{*}\,. \quad (6)$$

Now, we focus on the divergent terms for $\mathbf{G}=\mathbf{0}$ at the Γ-point of the Brillouin zone, $\mathbf{k}\to 0$. We start by analyzing the head of the polarizability, $\chi_{\mathbf{00}}^{0}(\mathbf{q},i\omega)$. Note that $A_{\mathbf{0},\mathbf{q}}^{i\mathbf{k},a\mathbf{k}-\mathbf{q}}\xrightarrow{\mathbf{q}\to 0}i\mathbf{q}\,\langle i\mathbf{k}|\mathbf{r}|a\mathbf{k}\rangle$ for $\mathbf{q}\to 0$ which can be seen by Taylor expansion of $e^{i\mathbf{q}\mathbf{r}}$ for small $\mathbf{q}$ and the orthogonality of molecular orbitals, $\langle i\mathbf{k}|a\mathbf{k}\rangle = 0$.[45,60] Therefore, $\chi_{\mathbf{00}}^{0}(\mathbf{q},i\omega)=O(|\mathbf{q}|^2)$ holds for small $\mathbf{q}$ and $\epsilon_{\mathbf{00}}(\mathbf{q},i\omega)$ remains finite for $\mathbf{q}\to 0$. For $\mathbf{q}\to 0$, the head, $W_{\mathbf{00}}^{\mathrm{c}}(\mathbf{q})$ and the wings, $W_{\mathbf{G0}}^{\mathrm{c}}(\mathbf{q})$, $W_{\mathbf{0G}'}^{\mathrm{c}}(\mathbf{q})$ diverge as $1/q^2$ and $1/q$, respectively, see Eq. (4). At the same time $A_{\mathbf{0},\mathbf{q}}^{n\mathbf{k},n\mathbf{k}-\mathbf{q}}\xrightarrow{\mathbf{q}\to 0}1$ and therefore, the entire expression for the Brillouin zone sampling in Eq. (2) diverges as $1/q^2$ for small q.

In the limit of very fine *k*-point sampling, we have $\sum_{\mathbf{q}}f(q)\to\Omega/(2\pi)^3\int dq\,4\pi q^2 f(q)$ such that the divergent terms $f(q)=1/q^2$ and $f(q)=1/q$ can be integrated. Thus, the Brilluoin zone sampling of the head and wings of W^{c} in Eq. (2) converge to a finite value when increasing the *k*-point mesh. The Γ-point has to be excluded from the *k*-point sampling of the head and the wings of W^{c} due to the division by 0 in Eq. (4). In the case of a finite *k*-point mesh with a distance $1/L = \sqrt[3]{1/\Omega}$ of the Γ-point to other *k*-points, the integration of the head $W_{\mathbf{00}}^{\mathrm{c}}(\mathbf{q})$ in Eq. (2) for the Γ-point, scales as

$$\int_{B_{1/L}(\mathbf{0})}d^3\mathbf{q}\,\frac{1}{q^2} = 4\pi\int_0^{1/L}dq = \frac{4\pi}{L}\,, \quad (7)$$

where we used the notation $B_r(\mathbf{0})$ for the sphere in the Brillouin zone with radius r around the Γ-point. We miss the $1/L$-scaling $\mathbf{G}=0$ terms of W^{c} in our Γ-point implementation with Gaussian basis functions. This results in a slow convergence of $1/L$ for *GW* quasiparticles with the cell length L. To achieve a fast convergence of *GW* quasiparticle levels with the cell size, we derive a correction term for our Gaussian Γ-point *GW* implementation in this work.

B. Resolution of the identity with overlap metric

As in the *GW* implementation[23] in the CP2K package[61,62], canonical *GW* implementations in a localized basis[19,20,22] employ the resolution of the identity (RI) to reduce the computational scaling of *GW* from $O(N^6)$ to $O(N^4)$. In this section, we give the equations that are used for the RI. The following index notation has been adopted: i, j (a, b) refer to occupied (virtual) molecular orbitals (MOs) ψ; n, m to either occupied or virtual ones; $\mu, \nu, \lambda, \sigma$ to primary Gaussian basis functions ϕ and P, Q to auxiliary Gaussian RI basis functions φ. The primary basis functions ϕ_μ are employed to expand the KS orbitals while the RI basis $\{\varphi_P\}$ is used to expand *GW* quantities as the polarizability, dielectric function and the screened Coulomb interaction, as we show in Sec. II C.

In Γ-only *GW*, four-center Coulomb integrals

$$(ia|jb) = \int_{\Omega_{\mathrm{cell}}}d\mathbf{r}\int_{\mathbb{R}^3}d\mathbf{r}'\,\psi_i(\mathbf{r})\psi_a(\mathbf{r})\psi_j(\mathbf{r}')\psi_b(\mathbf{r}')v(\mathbf{r},\mathbf{r}') \quad (8)$$

are appearing where $v(\mathbf{r},\mathbf{r}') = 1/|\mathbf{r}-\mathbf{r}'|$ denotes the Coulomb potential. All KS orbitals $\psi_n(\mathbf{r})$ in Eq. (8) are periodically repeated Bloch states at the Γ-point where we drop the $\mathbf{k}=\mathbf{0}$ index. Within the RI approximation based on the overlap metric, these integrals are factorized to[63]

$$(ia|jb)_{\mathrm{RI}} = \sum_{PQRS}(iaP)S_{PQ}^{-1}V_{QR}S_{RS}^{-1}(Sjb)\,. \quad (9)$$

The resolution of the identity can be seen as inserting $\mathrm{Id} = \sum_{PQ}|P\rangle S_{PQ}^{-1}\langle Q|$ twice into Eq. (8) which is exact in the limit of a complete RI basis $\{P\}$. Here, the overlap matrix $\mathbf{S}$ in the RI basis,[64]

$$S_{PQ} = \int_{\mathbb{R}^3}d\mathbf{r}\,\varphi_P^{\mathrm{P}}(\mathbf{r})\varphi_Q(\mathbf{r}) \quad (10)$$

is appearing since the Gaussian RI basis is non-orthogonal. The superscript P indicates that the functions are periodically repeated for condensed phase systems,

$$\varphi_Q^{\mathrm{P}}(\mathbf{r}) = \sum_i \varphi_Q(\mathbf{r} - \mathbf{R}_i), \qquad (11)$$

where $\mathbf{R}_i$ are the lattice vectors and φ_Q is a Gaussian basis function being localized on a single atom. Further, $\mathbf{V}$ denotes the Coulomb matrix in the RI basis,

$$V_{PQ} = \int_{\Omega_{\mathrm{cell}}} d\mathbf{r} \int_{\mathbb{R}^3} d\mathbf{r}' \varphi_P^{\mathrm{P}}(\mathbf{r}) \varphi_Q^{\mathrm{P}}(\mathbf{r}') v(\mathbf{r}, \mathbf{r}'). \qquad (12)$$

In practice, we compute the RI-Coulomb matrix by Ewald summation[65,66]

$$V_{PQ} = \sum_{\mathbf{G}>0} \frac{\varphi_P(\mathbf{G})\varphi_Q(\mathbf{G})}{|\mathbf{G}|^2}. \qquad (13)$$

We refer to the computation of Coulomb matrix elements in Eq. (13) as Gaussian and Plane Waves method which is commonly used for the Hartree energy[67] and for wavefunction correlation methods[68–74]. The $\mathbf{G} = 0$ component is excluded from Eq. (13) due to a divergence for s-type basis functions P, Q with $\varphi_{P,Q}(\mathbf{G}=0) \neq 0$. The three-center overlap integrals $(\mu\nu P)$ are given by[64]

$$(\mu\nu P) = \int_{\mathbb{R}^3} d\mathbf{r} \, \phi_\mu^{\mathrm{P}}(\mathbf{r}) \phi_\nu^{\mathrm{P}}(\mathbf{r}) \varphi_P(\mathbf{r}). \qquad (14)$$

The three-center overlap integrals (iaP) in Eq. (9) can be computed from Eq. (14) by

$$(iaP) = \sum_{\mu\nu} C_{\mu i} C_{\nu a} (\mu\nu P) \qquad (15)$$

where the MO coefficients $C_{\mu n}$ are obtained from the expansion of MOs in the primary Gaussian basis from KS DFT

$$\psi_n(\mathbf{r}) = \sum_\mu C_{\mu n} \phi_\mu^{\mathrm{P}}(\mathbf{r}). \qquad (16)$$

The RI factorization from Eq. (9) can be expressed in a compact form as

$$(ia|jb)_{\mathrm{RI}} = \sum_P B_P^{ia} B_P^{jb}, \qquad (17)$$

where the vector $\mathbf{b}^{ia}$ is given by

$$B_P^{ia} = \sum_{QR} (iaQ) S_{QR}^{-1} L_{RP}, \qquad (18)$$

where $\mathbf{L}$ is the Cholesky decomposition of $\mathbf{V}$ from Eq. (13),

$$\mathbf{V} = \mathbf{L}\mathbf{L}^\dagger. \qquad (19)$$

For later use, we define $\mathbf{a}^{ia}$ by

$$A_P^{ia} = \sum_Q (iaQ) S_{QP}^{-1}. \qquad (20)$$

C. Screened Coulomb interaction, dielectric matrix and polarizability in the RI basis

In this section, we rewrite the self-energy in a Gaussian basis to match the formulas in a plane-waves basis. For expanding GW quantities as the polarizability, the dielectric function and the screened Coulomb interaction, we employ the Gaussian RI basis from Sec. II B. This is the key to adopt the periodic correction from plane-waves GW to GW in a Gaussian basis.

As in Eq. (1), we compute the G_0W_0 quasiparticle energies in a Gaussian basis by

$$\varepsilon_n^{G_0W_0} = \varepsilon_n^{\mathrm{DFT}} + Z_n \mathrm{Re} \langle n|\Sigma_n^{\mathrm{c}}(\varepsilon_n^{\mathrm{DFT}}) + \Sigma^{\mathrm{x}} - V_{\mathrm{DFT}}^{\mathrm{xc}}|n\rangle \qquad (21)$$

where we have dropped the k-point index for a Γ-only implementation. The correlation part of the self-energyis is calculated for imaginary frequencies and analytically continued to real energies.[20,33,53,75–80] In a Gaussian basis, the correlation self-energy can be computed as[20,23,77]

$$\begin{aligned} \Sigma_n^{\mathrm{c}}(i\omega) = &-\frac{1}{2\pi} \sum_m \int_{-\infty}^\infty d\omega' \frac{1}{i(\omega-\omega') + \varepsilon_{\mathrm{F}} - \varepsilon_m} \\ &\times \sum_{PQ} B_P^{nm} \left[[1 - \Pi(i\omega')]_{PQ}^{-1} - \delta_{PQ} \right] B_Q^{mn}, \end{aligned} \qquad (22)$$

where

$$\Pi_{PQ}(i\omega) = 2 \sum_{ia} B_P^{ia} \frac{\varepsilon_i - \varepsilon_a}{\omega^2 + (\varepsilon_i - \varepsilon_a)^2} B_Q^{ia}. \qquad (23)$$

Inserting Eq. (18) into Eq. (22) and using the definition in Eq. (20) yields

$$\begin{aligned} \Sigma_n^{\mathrm{c}}(i\omega) = &-\frac{1}{2\pi} \sum_m \int_{-\infty}^\infty d\omega' \frac{1}{i(\omega-\omega') + \varepsilon_{\mathrm{F}} - \varepsilon_m} \\ &\times \sum_{PQ} A_P^{nm} W_{PQ}^{\mathrm{c}}(i\omega') A_Q^{mn}, \end{aligned} \qquad (24)$$

where the correlation part of the screened Coulomb potential $\mathbf{W}^{\mathrm{c}}(i\omega)$ is expanded in the Gaussian RI basis,

$$W_{PQ}^{\mathrm{c}}(i\omega) = \sum_{RT} L_{PR} \left[\epsilon_{RT}^{-1}(i\omega) - \delta_{RT} \right] L_{TQ}^\dagger, \qquad (25)$$

and the symmetric dielectric matrix $\boldsymbol{\epsilon}(i\omega)$ in the RI basis is given by $\boldsymbol{\epsilon}(i\omega) = \mathbf{1} - \boldsymbol{\Pi}(i\omega)$ with elements

$$\epsilon_{PQ}(i\omega) = \delta_{PQ} - \sum_{ia} \sum_{RT} L_{PR}^\dagger A_R^{ia} \frac{2(\varepsilon_i - \varepsilon_a)}{\omega^2 + (\varepsilon_i - \varepsilon_a)^2} A_T^{ia} L_{TQ}, \qquad (26)$$

where we have used Eq. (18), (20) and (23). In matrix notation, we have

$$\boldsymbol{\epsilon}(i\omega) = \mathbf{1} - \mathbf{L}^\dagger \chi^0(i\omega)\mathbf{L} \qquad (27)$$

and the polarizability $\chi^0(i\omega)$ in the RI basis with elements $\chi^0_{PQ}(i\omega)$ reads

$$\chi^0_{PQ}(i\omega) = \sum_{ia} A_P^{ia} \frac{2(\varepsilon_i - \varepsilon_a)}{\omega^2 + (\varepsilon_i - \varepsilon_a)^2} A_Q^{ia}. \qquad (28)$$

As it can be seen by comparing Eq. (24) and (2), as well as Eq. (28) and (6), the RI basis $\{\varphi_P\}$ corresponds to a plane-waves basis in plane-waves GW. We neglect the $\mathbf{G} = 0$ component when computing the bare Coulomb interaction in the RI basis in Eq. (13) and thus our RI basis only spans the subspace of plane waves with $|\mathbf{G}| > 0$. For a correction that removes the slow $1/L$ convergence of GW with the cell size L from Sec. II A, we add the $\mathbf{G} = 0$ function as additional function to the RI basis, as we show in the following section.

D. Setting the G = 0 component of Gaussian RI basis functions to zero and adding a single G = 0 function to the RI basis

Following the discussion at the end of the last section, we describe in this section how to add the $\mathbf{G} = 0$ function to the Gaussian RI basis.

Consider N_{aux} Gaussian RI basis functions $\varphi_1, \ldots, \varphi_{N_{\text{aux}}}$ where all Gaussian RI functions exhibit a vanishing $\mathbf{G} = 0$ component. This redefinition does not affect the GW results since the $\mathbf{G} = 0$ component is not used, see Eq. (13). Now, we add the $\mathbf{G} = 0$ function to the RI basis and the new RI basis consists of $N_{\text{aux}} + 1$ functions $\varphi_0, \varphi_1, \ldots, \varphi_{N_{\text{aux}}}$, where φ_0 is the $\mathbf{G} = 0$ function which is a normalized constant in real space,

$$\varphi_0(\mathbf{r}) = \Omega_{\text{cell}}^{-1/2} \delta_{\mathbf{r} \in \Omega_{\text{cell}}}. \qquad (29)$$

Then, the Γ-only overlap matrix $\mathbf{S}$ reads

$$\mathbf{S} \equiv \begin{pmatrix} S_{\text{head}} & \mathbf{S}_{\text{wings}} \\ \mathbf{S}^\dagger_{\text{wings}} & \mathbf{S}_{\text{body}} \end{pmatrix} = \begin{pmatrix} 1 & \mathbf{0} \\ \mathbf{0} & \mathbf{S}_{\text{body}} \end{pmatrix} \qquad (30)$$

where $\mathbf{S}_{\text{body}}$ is the overlap matrix of the Gaussian RI basis. The wings of $\mathbf{S}$ are zero since, according to the redefinition from above, all RI Gaussian basis functions $P \in [1, N_{\text{aux}}]$ do not exhibit a $\mathbf{G} = 0$ component:

$$S_{0P} = S_{P0} = \sum_{\mathbf{G}} \varphi_0(\mathbf{G}) \varphi_P(\mathbf{G}) = 0. \qquad (31)$$

E. k-dependent polarizability, dielectric function and screened Coulomb interaction

In this section, we expand the polarizability, the dielectric function and the screened Coulomb interaction in the Gaussian RI basis with additional $\mathbf{G} = 0$ function from Sec. II D. Moreover, we adopt k-points for head and wing elements from plane-waves GW, see Sec. II A.

We start with the polarizability using Γ-only for the body[53]

$$\chi^0(i\omega, \mathbf{k}) = \begin{pmatrix} \chi^0_{\text{head}}(i\omega, \mathbf{k}) & \chi^0_{\text{wings}}(i\omega, \mathbf{k}) \\ \left(\chi^0_{\text{wings}}(i\omega, \mathbf{k})\right)^\dagger & \chi^0_{\text{body}}(i\omega) \end{pmatrix}. \qquad (32)$$

Omitting the integration over the first Brillouin zone for the polarizability, its head is given by Eq. (6)

$$\chi^0_{00}(i\omega, \mathbf{k}) = \frac{1}{\Omega_{\text{cell}}} \sum_{ia} \frac{2(\varepsilon_i - \varepsilon_a)}{\omega^2 + (\varepsilon_i - \varepsilon_a)^2} \left| \langle \psi_{i\mathbf{0}} | e^{i\mathbf{k}\mathbf{r}} | \psi_{a-\mathbf{k}} \rangle \right|^2. \qquad (33)$$

The prefactor $1/\Omega_{\text{cell}}$ results from the normalization of $\varphi_0(\mathbf{r})$ from Eq. (29). The wings are given by

$$\chi^0_{0Q}(i\omega, \mathbf{k}) = \frac{1}{\Omega_{\text{cell}}^{1/2}} \sum_{ia} A_Q^{ia} \frac{2(\varepsilon_i - \varepsilon_a)}{\omega^2 + (\varepsilon_i - \varepsilon_a)^2} \langle \psi_{i\mathbf{0}} | e^{i\mathbf{k}\mathbf{r}} | \psi_{a-\mathbf{k}} \rangle \qquad (34)$$

using the Γ-point for the RI basis function Q, cf. Eq. (6) and (28).

The dielectric matrix from Eq. (27) for k-points is given by

$$\boldsymbol{\epsilon}(i\omega, \mathbf{k}) \overset{(5)}{=} \mathbf{1} - \mathbf{L}^\dagger(\mathbf{k}) \chi^0(i\omega, \mathbf{k}) \mathbf{L}(\mathbf{k}), \qquad (35)$$

where $\mathbf{L}(\mathbf{k})$ is the Cholesky decomposition of the Coulomb matrix

$$\mathbf{V}(\mathbf{k}) \equiv \begin{pmatrix} V_{\text{head}}(\mathbf{k}) & \mathbf{0} \\ \mathbf{0} & \mathbf{V}_{\text{body}} \end{pmatrix} = \mathbf{L}(\mathbf{k}) \mathbf{L}^\dagger(\mathbf{k}). \qquad (36)$$

The elements of $\mathbf{V}(\mathbf{k})$ are given by[45,64]

$$V_{00}(\mathbf{k}) = \frac{4\pi}{|\mathbf{k}|^2}, \qquad V_{PQ} = \sum_{\mathbf{G} > 0} \frac{\varphi_P(\mathbf{G}) \varphi_Q(\mathbf{G})}{|\mathbf{G}|^2}, \qquad (37)$$

which are well-defined for $\mathbf{k} \neq 0$. The wings of $\mathbf{V}(\mathbf{k})$ vanish since $\varphi_0(\mathbf{G}) = \delta_{\mathbf{G}, \mathbf{0}}$ and $\varphi_P(\mathbf{G} = 0) = 0$ for the remaining Gaussian RI functions. For $\mathbf{V}_{\text{body}}$, only the Γ point is used. Then, the Cholesky decomposition $\mathbf{L}(\mathbf{k})$ of $\mathbf{V}(\mathbf{k})$ reads

$$\mathbf{L}(\mathbf{k}) = \begin{pmatrix} \sqrt{4\pi}/|\mathbf{k}| & \mathbf{0} \\ \mathbf{0} & \mathbf{L}_{\text{body}} \end{pmatrix}, \qquad (38)$$

where $\mathbf{L}_{\text{body}}$ is the Cholesky decomposition of the body Coulomb matrix $\mathbf{V}_{\text{body}}$.

The head, wings and the body of the dielectric matrix from Eq. (35) are defined as

$$\boldsymbol{\epsilon}(i\omega, \mathbf{k}) \equiv \begin{pmatrix} \epsilon_{\text{head}}(i\omega, \mathbf{k}) & \boldsymbol{\epsilon}_{\text{wings}}(i\omega, \mathbf{k}) \\ \boldsymbol{\epsilon}^\dagger_{\text{wings}}(i\omega, \mathbf{k}) & \boldsymbol{\epsilon}_{\text{body}}(i\omega) \end{pmatrix} \qquad (39)$$

and read when using Eq. (32) and (38)

$$\epsilon_{\text{head}}(i\omega, \mathbf{k}) = 1 - 4\pi \chi^0_{\text{head}}(i\omega, \mathbf{k})/|\mathbf{k}|^2, \qquad (40)$$

$$\boldsymbol{\epsilon}_{\text{wings}}(i\omega, \mathbf{k}) = -\sqrt{4\pi} \chi^0_{\text{wings}}(i\omega, \mathbf{k}) \mathbf{L}_{\text{body}}/|\mathbf{k}|, \qquad (41)$$

$$\boldsymbol{\epsilon}_{\text{body}}(i\omega) = \mathbf{1} - \mathbf{L}^\dagger_{\text{body}} \chi^0_{\text{body}}(i\omega) \mathbf{L}_{\text{body}}. \qquad (42)$$

Its inverse $\boldsymbol{\epsilon}^{\text{inv}}(i\omega, \mathbf{k})$ is given by (for $\mathbf{k} \neq \mathbf{0}$)

$$\boldsymbol{\epsilon}^{\text{inv}}(i\omega, \mathbf{k}) \equiv \begin{pmatrix} \epsilon^{\text{inv}}_{\text{head}}(i\omega, \mathbf{k}) & \boldsymbol{\epsilon}^{\text{inv}}_{\text{wings}}(i\omega, \mathbf{k}) \\ \boldsymbol{\epsilon}^{\text{inv},\dagger}_{\text{wings}}(i\omega, \mathbf{k}) & \boldsymbol{\epsilon}^{\text{inv}}_{\text{body}}(i\omega, \mathbf{k}) \end{pmatrix} := \boldsymbol{\epsilon}^{-1}(i\omega, \mathbf{k}), \qquad (43)$$

where its elements are given by inverting Eq. (39)

$$\epsilon_{\text{head}}^{\text{inv}}(i\omega, \mathbf{k}) = 1/[\epsilon_{\text{head}}(i\omega, \mathbf{k}) - \boldsymbol{\epsilon}_{\text{wings}}(i\omega, \mathbf{k})$$
$$\times \boldsymbol{\epsilon}_{\text{body}}^{-1}(i\omega)\boldsymbol{\epsilon}_{\text{wings}}^{\dagger}(i\omega, \mathbf{k})] . \tag{44}$$

$$\boldsymbol{\epsilon}_{\text{wings}}^{\text{inv}}(i\omega, \mathbf{k}) = - \epsilon_{\text{head}}^{\text{inv}}(i\omega, \mathbf{k})\boldsymbol{\epsilon}_{\text{wings}}(i\omega, \mathbf{k})\boldsymbol{\epsilon}_{\text{body}}^{-1}(i\omega) \tag{45}$$

$$\boldsymbol{\epsilon}_{\text{body}}^{\text{inv}}(i\omega, \mathbf{k}) = \boldsymbol{\epsilon}_{\text{body}}^{-1}(i\omega) + \epsilon_{\text{head}}^{\text{inv}}(i\omega, \mathbf{k})\boldsymbol{\epsilon}_{\text{body}}^{-1}(i\omega)$$
$$\times \boldsymbol{\epsilon}_{\text{wings}}^{\dagger}(i\omega, \mathbf{k})\boldsymbol{\epsilon}_{\text{wings}}(i\omega, \mathbf{k})\boldsymbol{\epsilon}_{\text{body}}^{-1}(i\omega) . \tag{46}$$

Analogously to Eq. (4) and Eq. (25), we obtain $\mathbf{W}^{\text{c}}(i\omega, \mathbf{k})$ for $\mathbf{k} \neq \mathbf{0}$ as

$$\mathbf{W}^{\text{c}}(i\omega, \mathbf{k}) = \mathbf{L}(\mathbf{k})(\boldsymbol{\epsilon}^{\text{inv}}(i\omega, \mathbf{k}) - \mathbf{1})\mathbf{L}^{\dagger}(\mathbf{k}) \tag{47}$$

$$= \begin{pmatrix} 4\pi(\epsilon_{\text{head}}^{\text{inv}}(i\omega, \mathbf{k}) - 1)/|\mathbf{k}|^2 & \sqrt{4\pi}\,\boldsymbol{\epsilon}_{\text{wings}}^{\text{inv}}(i\omega, \mathbf{k})\mathbf{L}_{\text{body}}/|\mathbf{k}| \\ \sqrt{4\pi}\,\mathbf{L}_{\text{body}}^{\dagger}\boldsymbol{\epsilon}_{\text{wings}}^{\text{inv},\dagger}(i\omega, \mathbf{k})/|\mathbf{k}| & \mathbf{L}_{\text{body}}^{\dagger}(\boldsymbol{\epsilon}_{\text{body}}^{\text{inv}}(i\omega, \mathbf{k}) - 1)\mathbf{L}_{\text{body}} \end{pmatrix} . \tag{48}$$

F. k-point sampling for the self-energy in the limit of $k \to 0$

In order to identify, which contributions have to be taken into account for the correction in periodic GW in a Gaussian basis, we examine the behaviour of the k-point sum in the self-energy at the Γ-point, $\mathbf{k} \to 0$.

Comparing Eq. (2) and Eq. (24) and assuming flat bands ($\varepsilon_{m\mathbf{q}} = \varepsilon_m$), we obtain:

$$\Sigma_n^{\text{c}}(i\omega) = - \frac{1}{2\pi} \sum_m \int_{-\infty}^{\infty} d\omega' \frac{1}{i(\omega - \omega') + \varepsilon_{\text{F}} - \varepsilon_m}$$
$$\times \frac{1}{N_{\mathbf{k}}} \sum_{\mathbf{k} \neq 0} \sum_{PQ} A_{P\mathbf{k}}^{n\mathbf{0}, m-\mathbf{k}} W_{PQ}^{\text{c}}(i\omega, \mathbf{k}) \left(A_{Q\mathbf{k}}^{n\mathbf{0}, m-\mathbf{k}} \right)^* . \tag{49}$$

The summation over the RI indices P, Q include the summation over the $\mathbf{G} = 0$ RI function. Due to the divergence of the head $W_{00}^{\text{c}}(i\omega, \mathbf{k})$ and the wings, $W_{P0}^{\text{c}}(i\omega, \mathbf{k})$ and $W_{0Q}^{\text{c}}(i\omega, \mathbf{k})$, for $\mathbf{k} \to 0$, the Γ point is excluded from the summation. The three-center overlap integrals in the limit of small $\mathbf{k}$ for the $\mathbf{G} = 0$ RI function are given by[45,60]

$$A_{0\mathbf{k}}^{n\mathbf{0}, n-\mathbf{k}} = \langle \psi_{n\mathbf{0}} | e^{i\mathbf{k}\mathbf{r}} | \psi_{n-\mathbf{k}} \rangle \stackrel{\mathbf{k}\to 0}{=} 1 + i\mathbf{k}\langle \psi_{n\mathbf{0}} | \mathbf{r} | \psi_{n\mathbf{0}} \rangle , \tag{50}$$

$$A_{0\mathbf{k}}^{n\mathbf{0}, m-\mathbf{k}} = \langle \psi_{n\mathbf{0}} | e^{i\mathbf{k}\mathbf{r}} | \psi_{m-\mathbf{k}} \rangle \stackrel{\mathbf{k}\to 0}{\underset{n\neq m}{=}} i\mathbf{k}\langle \psi_{n\mathbf{0}} | \mathbf{r} | \psi_{m\mathbf{0}} \rangle , \tag{51}$$

Then, the sum over RI basis functions in Eq. (49) for $n = m$ using the matrix-vector notation with the row vector $(\mathbf{a}^{nn}(\mathbf{k}))_P = A_{P\mathbf{k}}^{n\mathbf{0}, m-\mathbf{k}}$ in the limit $\mathbf{k} \to 0$ turns into

$$\mathbf{a}^{nn}(\mathbf{k})\mathbf{W}^{\text{c}}(i\omega, \mathbf{k}) (\mathbf{a}^{nn}(\mathbf{k}))^{\dagger} \stackrel{\mathbf{k}\to 0}{=}$$

$$\stackrel{(50)}{=} \left(1 + i\mathbf{k}\langle \psi_{n\mathbf{0}} | \mathbf{r} | \psi_{n\mathbf{0}} \rangle \quad \mathbf{a}_{\text{body}}^{nn} \right) \begin{pmatrix} 4\pi(\epsilon_{\text{head}}^{\text{inv}}(i\omega, \mathbf{k}) - 1)/|\mathbf{k}|^2 & \sqrt{4\pi}\,\boldsymbol{\epsilon}_{\text{wings}}^{\text{inv}}(i\omega, \mathbf{k})\mathbf{L}_{\text{body}}/|\mathbf{k}| \\ \sqrt{4\pi}\,\mathbf{L}_{\text{body}}^{\dagger}\boldsymbol{\epsilon}_{\text{wings}}^{\text{inv},\dagger}(i\omega, \mathbf{k})/|\mathbf{k}| & \mathbf{L}_{\text{body}}^{\dagger}(\boldsymbol{\epsilon}_{\text{body}}^{\text{inv}}(i\omega, \mathbf{k}) - 1)\mathbf{L}_{\text{body}} \end{pmatrix} \begin{pmatrix} 1 - i\mathbf{k}\langle \psi_{n\mathbf{0}} | \mathbf{r} | \psi_{n\mathbf{0}} \rangle \\ (\mathbf{a}_{\text{body}}^{nn})^{\text{T}} \end{pmatrix} \tag{52}$$

$$= \frac{4\pi}{|\mathbf{k}|^2} (\epsilon_{\text{head}}^{\text{inv}}(i\omega, \mathbf{k}) - 1) - \frac{\sqrt{4\pi}}{|\mathbf{k}|^1} \text{Re}\left(2\boldsymbol{\epsilon}_{\text{wings}}^{\text{inv}}(i\omega, \mathbf{k})\mathbf{L}_{\text{body}}(\mathbf{a}_{\text{body}}^{nn})^{\text{T}} \right) + O\left(\frac{1}{|\mathbf{k}|^0} \right) = \frac{4\pi}{|\mathbf{k}|^2} (\epsilon_{\text{head}}^{\text{inv}}(i\omega, \mathbf{k}) - 1) + O\left(\frac{1}{|\mathbf{k}|^0} \right) . \tag{53}$$

The $1/|\mathbf{k}|^1$ term in Eq. (53) vanishes due to $\text{Re}(\boldsymbol{\epsilon}_{\text{wings}}^{\text{inv}}(i\omega, \mathbf{k})) = 0$ for $\mathbf{k} \to 0$ [see Eqs. (45), (42), and (34)] and $\text{Im}(\mathbf{L}_{\text{body}}(\mathbf{a}_{\text{body}}^{nn})^{\text{T}}) = 0$. Therefore, a correction due to wing contributions of W^{c} seems to be of minor importance compared to the head when using a Gaussian basis.

For the contraction with $n \neq m$ in Eq. (49), we have

$$\mathbf{a}^{nm}(\mathbf{k})\mathbf{W}^{\text{c}}(i\omega, \mathbf{k}) (\mathbf{a}^{nm}(\mathbf{k}))^{\dagger} \stackrel{(51)}{=} O(1/|\mathbf{k}|^0) . \tag{54}$$

Therefore, we do not include $A_{0\mathbf{k}}^{n\mathbf{0}, m-\mathbf{k}}$ matrix elements with $n \neq m$ from Eq. (49) in the periodic correction scheme.

Then, the k-point sum for the periodic correction from Eq. (49) only includes the head of $\mathbf{W}^{\text{c}}$ and matrix elements $A_{0\mathbf{k}}^{n\mathbf{0}, n-\mathbf{k}}$ with $n = m$:

$$\sum_{mPQ} \sum_{\mathbf{k} \neq 0} A_{P\mathbf{k}}^{n\mathbf{0}, m-\mathbf{k}} W_{PQ}^{\text{c}}(i\omega, \mathbf{k}) \left(A_{Q\mathbf{k}}^{n\mathbf{0}, m-\mathbf{k}} \right)^*$$
$$= \sum_{\mathbf{k} \neq 0} \frac{4\pi}{|\mathbf{k}|^2} \left(\epsilon_{\text{head}}^{\text{inv}}(i\omega, \mathbf{k}) - 1 \right) \left| \langle \psi_{n\mathbf{0}} | e^{i\mathbf{k}\mathbf{r}} | \psi_{n-\mathbf{k}} \rangle \right|^2 + O\left(\frac{1}{|\mathbf{k}|^0} \right) . \tag{55}$$

The divergence $1/|\mathbf{k}|^2$ in Eq. (55) is integrable, as discussed in Sec. II A.

G. Algorithm of the correction scheme for periodic GW with Gaussians

1. Setup a $\mathbf{k}$-point mesh excluding the Γ-point.

2. Compute $\chi^0_{\text{head}}(i\omega, \mathbf{k})$ according to Eq. (33):

$$\chi^0_{\text{head}}(i\omega, \mathbf{k}) = \frac{1}{\Omega_{\text{cell}}} \sum_{ia} \frac{2(\varepsilon_i - \varepsilon_a)}{\omega^2 + (\varepsilon_i - \varepsilon_a)^2} \left| \langle \psi_{i\mathbf{0}} | e^{i\mathbf{k}\mathbf{r}} | \psi_{a-\mathbf{k}} \rangle \right|^2,$$

(56)

According to what has been discussed in the previous section, we assume the wings to have a small contribution and we exclude their computation.

3. Compute the head of the dielectric matrix from Eq. (42):

$$\epsilon_{\text{head}}(i\omega, \mathbf{k}) = 1 - 4\pi \chi^0_{\text{head}}(i\omega, \mathbf{k})/|\mathbf{k}|^2 . \qquad (57)$$

4. Compute the head of the inverse dielectric matrix $\boldsymbol{\epsilon}^{\text{inv}}$ according to Eq. (44) with neglecting wing contributions:

$$\epsilon^{\text{inv}}_{\text{head}}(i\omega, \mathbf{k}) = 1/\epsilon_{\text{head}}(i\omega, \mathbf{k}) . \qquad (58)$$

5. Compute the correction term $\Delta_{nn}(i\omega)$ appearing from the head of W^c in $1/\Omega \sum_{\mathbf{k}} \mathbf{a}^{nm}(\mathbf{k}) W^c(i\omega, \mathbf{k}) (\mathbf{a}^{nm}(\mathbf{k}))^\dagger$ in Eq. (49) according to Eq. (55) as:

$$\Delta_{nn}(i\omega) = \frac{4\pi}{\Omega} \sum_{\mathbf{k} \neq 0} \frac{\epsilon^{\text{inv}}_{\text{head}}(i\omega, \mathbf{k}) - 1}{|\mathbf{k}|^2} \left| \langle \psi_{n\mathbf{0}} | e^{i\mathbf{k}\mathbf{r}} | \psi_{n-\mathbf{k}} \rangle \right|^2 . \quad (59)$$

Then, the Γ-only correlation self-energy from Eq. (22) including the correction term $\Delta_{nn}(i\omega)$ reads

$$\Sigma^c_n(i\omega) = -\frac{1}{2\pi} \sum_m \int_{-\infty}^{\infty} d\omega' \frac{1}{i(\omega - \omega') + \varepsilon_F - \varepsilon_m}$$

$$\times \left[\sum_{PQ} B^{nm}_P \left[[1 - \Pi(i\omega')]^{-1}_{PQ} - \delta_{PQ} \right] B^{mn}_Q + \Delta_{nn}(i\omega') \delta_{nm} \right].$$

(60)

III. BENCHMARK CALCULATIONS

A. Computational details

For all calculations reported here, we employ the Gaussian and plane waves scheme (GPW)[81] together with Goedecker-Teter-Hutter (GTH) type pseudopotentials[82,83] for the underlying generalized Kohn-Sham (KS) equations with the PBE functional[84] as implemented in CP2K[61,62,67,85,86]. For the exchange self-energy from Eq. (21), we employ a real-space truncation of the Coulomb interaction[49–51] with a truncation radius equal to half of the cell size.

For expanding the KS orbitals, we use correlation-consistent (cc) Gaussian basis sets[87,88] which are specifically designed for the use with GTH pseudopotentials. The basis set extrapolated GW results are obtained from the cc double-, triple- and quadrupole zeta split-valence quality basis sets by a linear regression against the inverse of the total number of basis functions.[21,23,33] The extrapolation in the basis set for

Reference	Diamond	Lithium hydride
This work	$5.48 \pm 0.06\,\text{eV}$	$4.66 \pm 0.04\,\text{eV}$
Ref. 99	$5.54\,\text{eV}$	–
Ref. 100	$5.55\,\text{eV}$	–
Ref. 101	$5.50\,\text{eV}$	–
Ref. 102	–	$4.75\,\text{eV}$
Experiment[101,103]	$5.48\,\text{eV}$	$4.99\,\text{eV}$

TABLE I. G_0W_0@PBE HOMO-LUMO gaps and measured fundamental gaps of diamond and LiH from the literature.

KS orbitals typically results in statistical errors below $0.1\,\text{eV}$ for GW quasiparticle levels.[33]

The Gaussian RI basis set is used for expanding the screened Coulomb interaction and is designed for the use with a specific basis set for the KS orbitals, as described in Ref. 89. Typically, the convergence of GW quasiparticle energies with respect to the RI basis is fast such that an extrapolation is not necessary for the RI basis.

The Berry phase $\langle \phi_\mu | e^{i\mathbf{k}\mathbf{r}} | \phi_\nu \rangle$ in the Gaussian basis is available in standard quantum chemistry codes for calculating dipole moments in periodic systems[90–95]. To ensure numerical stability when computing the Berry phase in the Gaussian basis, we employ a non-diffuse auxiliary basis and project the MO coefficients into this subspace.[96,97] We employ $6\times6\times6$ and $12\times12\times12$ k-point meshes and extrapolate the results to the infinitely dense k-point mesh.

As benchmark systems, we employ solid Lithium hydride, diamond, and the molecular crystals build of ammonia and carbon dioxide molecules. For LiH and diamond, we employ the experimental lattice constants of $4.084\,\text{Å}$ and $3.567\,\text{Å}$, respectively. For both molecular crystals, we employ the geometry from Ref. 98.

B. Results

The basis-set extrapolated G_0W_0@PBE fundamental gaps as function of the cell size are shown in Fig. 1. We compare the results without correction [Eq. (21) together with Eq. (22), blue] with the results employing the correction [Eq. (21) together with Eq. (60), green].

For the uncorrected G_0W_0@PBE fundamental gaps (blue), we observe a slow $1/L$ convergence with the cell length L. The extrapolation with the inverse cell length yields the G_0W_0@PBE gaps of $4.66 \pm 0.04\,\text{eV}$ for LiH, $5.48 \pm 0.06\,\text{eV}$ for diamond, $7.49 \pm 0.11\,\text{eV}$ for the NH_3 crystal and $10.51 \pm 0.07\,\text{eV}$ for the CO_2 crystal. The statistical error includes both errors from basis set and the supercell extrapolation. These values are in good agreement with (indirect) fundamental gaps from the literature, see Table I. For both molecular crystals, we are not aware of fundamental gaps from the literature. We conclude that using basis set and supercell extrapolation, a Γ-only G_0W_0 implementation can give accurate fundamental gaps.

In practice, the extrapolation of the supercell can be impossible since the unit cell is already large if disordered systems
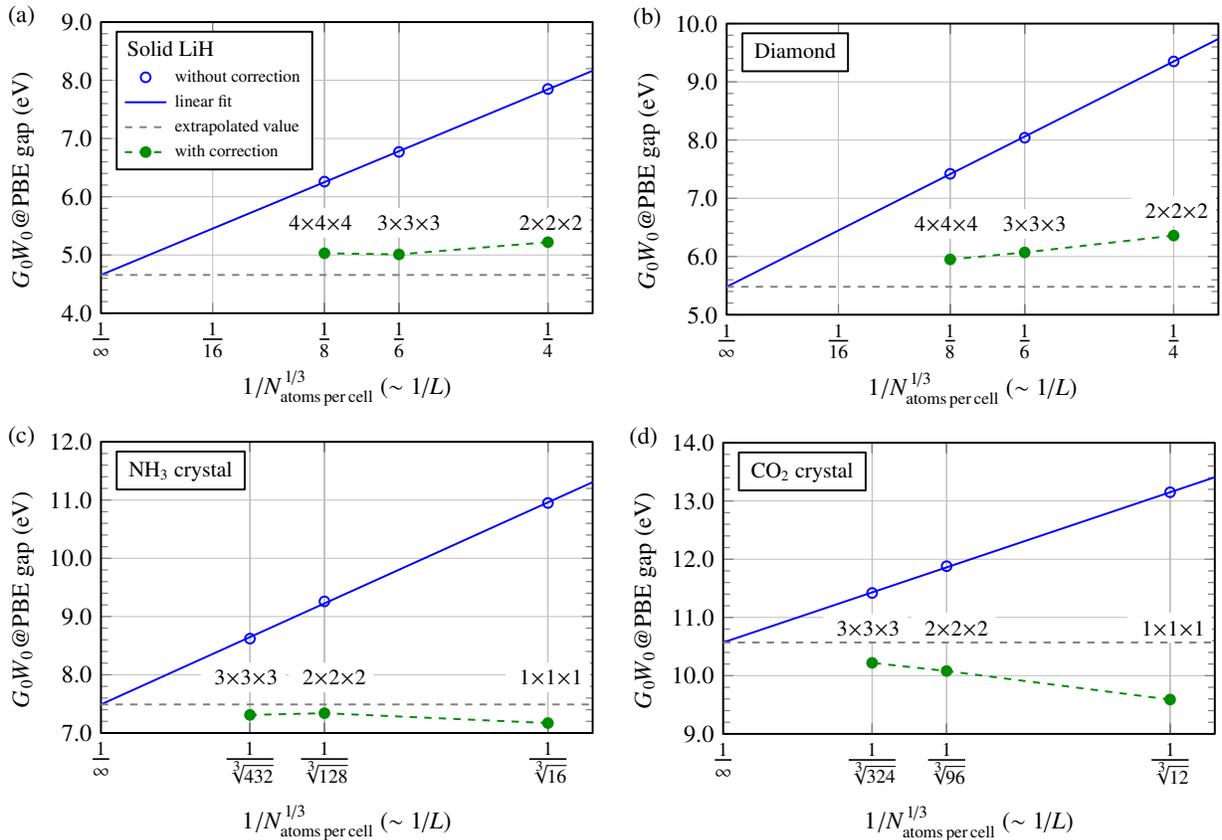
FIG. 1. Basis-set extrapolated G_0W_0@PBE fundamental gaps of solid Lithium hydride, diamond and the molecular crystals NH_3 and CO_2 as function of the supercell size. The blue circles are the gaps computed without the correction, see Eq. (21) together with Eq. (22), where the blue line represents the linear regression. The intersept of the regression line with the ordinate determines the supercell extrapolated gap which is indicated by the dashed gray line. By the green dots, we show the gaps being computed with the periodic correction from Eq. (21) together with Eq. (60) where the dashed green lines are simple connections of the data points to guide the eye. It is observed that the corrected gaps are much closer to the supercell extrapolated gap compared to the non-corrected gaps.

are considered, e.g. in molecular dynamics simulations[10,16,17]. For GW calculations of these systems, a periodic correction is necessary. In Fig. 1, we show the fundamental G_0W_0@PBE gaps when using our correction from Sec. II G. We observe that the gaps computed with the correction are a factor three to ten closer to the extrapolated gap than the non-correct ones. For the largest supercells which correspond to typical cells in molecular dynamics simulations, the corrected G_0W_0@PBE gaps are all within $0.5\,eV$ compared to the extrapolated values. This improves substantially compared to the uncorrected gaps and turns the Γ-only GW method in a Gaussian basis into a useful tool for computing quasiparticle levels in periodic, disordered systems where large unit cells are necessary.

IV. CONCLUSIONS

We have presented a correction scheme for periodic Γ-only GW calculations in a Gaussian basis. The correction is derived by adding the $\mathbf{G}=\mathbf{0}$ function to the resolution-of-the-identity (RI) basis. As a second step, we apply k-point sampling for

the correction mimicking an infinitely large cell for the head matrix elements, i.e. the diagonal elements corresponding to the $\mathbf{G}=\mathbf{0}$ function in the RI basis. For the benchmark systems solid Lithium hydride, diamond and two molecular crystals, the dependence of the corrected GW quasiparticle levels on the cell size is reduced by a factor of three to ten compared to GW calculations without correction. The correction scheme comes along with negligible computational cost and enables GW calculations for supercells containing hundreds of atoms with Gaussian basis functions.

* jan.wilhelm@chem.uzh.ch
1 G. Onida, L. Reining, and A. Rubio, Rev. Mod. Phys. **74**, 601 (2002).
2 W. Kohn and L. J. Sham, Phys. Rev. **140**, A1133 (1965).
3 L. Hedin, Phys. Rev. **139**, A796 (1965).
4 X. Ren, N. Marom, F. Caruso, M. Scheffler, and P. Rinke, Phys. Rev. B **92**, 081104 (2015).
5 C. Rostgaard, K. W. Jacobsen, and K. S. Thygesen, Phys. Rev. B **81**, 085103 (2010).
6 F. Caruso, M. Dauth, M. J. van Setten, and P. Rinke, J. Chem. Theory Comput. **12**, 5076 (2016).
7 P. Scherpelz, M. Govoni, I. Hamada, and G. Galli, J. Chem. Theory Comput. **12**, 3523 (2016).
8 M. S. Hybertsen and S. G. Louie, Phys. Rev. B **34**, 5390 (1986).
9 P. Umari, G. Stenuit, and S. Baroni, Phys. Rev. B **81**, 115104 (2010).
10 M. Govoni and G. Galli, J. Chem. Theory Comput. **11**, 2680 (2015).
11 F. Bruneval, J. Chem. Phys. **145**, 234110 (2016).
12 M. Shao, L. Lin, C. Yang, F. Liu, F. H. Da Jornada, J. Deslippe, and S. G. Louie, Sci. China Math. **59**, 1593 (2016).
13 H.-V. Nguyen, T. A. Pham, D. Rocca, and G. Galli, Phys. Rev. B **85**, 081101 (2012).
14 Y. Ping, D. Rocca, and G. Galli, Chem. Soc. Rev. **42**, 2437 (2013).
15 F. Giustino, M. L. Cohen, and S. G. Louie, Phys. Rev. B **81**, 115105 (2010).
16 A. P. Gaiduk, M. Govoni, R. Seidel, J. H. Skone, B. Winter, and G. Galli, J. Am. Chem. Soc. **138**, 6912 (2016).
17 D. Opalka, T. A. Pham, M. Sprik, and G. Galli, J. Phys. Chem. B **119**, 9651 (2015).
18 D. Opalka, T. Pham, M. Sprik, and G. Galli, J. Chem. Phys. **141**, 034501 (2014).
19 X. Blase, C. Attaccalite, and V. Olevano, Phys. Rev. B **83**, 115103 (2011).
20 X. Ren, P. Rinke, V. Blum, J. Wieferink, A. Tkatchenko, A. Sanfilippo, K. Reuter, and M. Scheffler, New J. Phys. **14**, 053020 (2012).
21 M. J. van Setten, F. Weigend, and F. Evers, J. Chem. Theory Comput. **9**, 232 (2013).
22 F. Bruneval, T. Rangel, S. M. Hamed, M. Shao, C. Yang, and J. B. Neaton, Comp. Phys. Comm. **208**, 149 (2016).
23 J. Wilhelm, M. Del Ben, and J. Hutter, J. Chem. Theory Comput. **12**, 3623 (2016).
24 M. Rohlfing, P. Krüger, and J. Pollmann, Phys. Rev. B **48**, 17791 (1993).
25 M. Rohlfing, P. Krüger, and J. Pollmann, Phys. Rev. B **52**, 1905 (1995).
26 D. Foerster, P. Koval, and D. Sánchez-Portal, J. Chem. Phys. **135**, 074105 (2011).
27 P. Koval, D. Foerster, and D. Sánchez-Portal, Phys. Rev. B **89**, 155417 (2014).
28 F. Kaplan, F. Weigend, F. Evers, and M. J. van Setten, J. Chem. Theory Comput. **11**, 5152 (2015).
29 F. Kaplan, M. E. Harding, C. Seiler, F. Weigend, F. Evers, and M. J. van Setten, J. Chem. Theory Comput. **12**, 2528 (2016).
30 F. Bruneval and M. A. L. Marques, J. Chem. Theory Comput. **9**, 324 (2013).
31 S. Körbel, P. Boulanger, I. Duchemin, X. Blase, M. A. L. Marques, and S. Botti, J. Chem. Theory Comput. **10**, 3934 (2014).
32 J. W. Knight, X. Wang, L. Gallandi, O. Dolgounitcheva, X. Ren, J. V. Ortiz, P. Rinke, T. Körzdörfer, and N. Marom, J. Chem. Theory Comput. **12**, 615 (2016).
33 M. J. van Setten, F. Caruso, S. Sharifzadeh, X. Ren, M. Scheffler, F. Liu, J. Lischner, L. Lin, J. R. Deslippe, S. G. Louie, C. Yang, F. Weigend, J. B. Neaton, F. Evers, and P. Rinke, J. Chem. Theory Comput. **11**, 5665 (2015).
34 T. Rangel, S. M. Hamed, F. Bruneval, and J. B. Neaton, J. Chem. Theory Comput. **12**, 2834 (2016).
35 N. Marom, T. Körzdörfer, X. Ren, A. Tkatchenko, and J. R. Chelikowsky, J. Phys. Chem. Lett. **5**, 2395 (2014).
36 N. Marom, J. Phys. Condens. Matter **29**, 103003 (2017).
37 C. Faber, P. Boulanger, C. Attaccalite, I. Duchemin, and X. Blase, Phil. Trans. R. Soc. A **372**, 20130271 (2014).
38 X. Blase, P. Boulanger, F. Bruneval, M. Fernandez-Serra, and I. Duchemin, J. Chem. Phys. **144**, 034109 (2016).
39 C. Faber, I. Duchemin, T. Deutsch, and X. Blase, Phys. Rev. B **86**, 155315 (2012).
40 X. Leng, J. Feng, T. Chen, C. Liu, and Y. Ma, Phys. Chem. Chem. Phys. **18**, 30777 (2016).
41 J. Deslippe, G. Samsonidze, D. A. Strubbe, M. Jain, M. L. Cohen, and S. G. Louie, Comput. Phys. Commun. **183**, 1269 (2012).
42 E. Maggio, P. Liu, M. J. van Setten, and G. Kresse, J. Chem. Theory Comput. **13**, 635 (2017).
43 D. Neuhauser, Y. Gao, C. Arntsen, C. Karshenas, E. Rabani, and R. Baer, Phys. Rev. Lett. **113**, 076402 (2014).
44 V. Vlček, E. Rabani, D. Neuhauser, and R. Baer, arXiv preprint arXiv:1612.08999 (2016).
45 C. Freysoldt, P. Eggert, P. Rinke, A. Schindlmayr, R. W. Godby, and M. Scheffler, Comp. Phys. Comm. **176**, 1 (2007).
46 J. McClain, Q. Sun, G. K.-L. Chan, and T. C. Berkelbach, J. Chem. Theory Comput. **13**, 1209 (2017).
47 Q. Sun, T. C. Berkelbach, N. S. Blunt, G. H. Booth, S. Guo, Z. Li, J. Liu, J. McClain, S. Sharma, S. Wouters, *et al.*, arXiv preprint arXiv:1701.08223 (2017).
48 F. Gygi and A. Baldereschi, Phys. Rev. B **34**, 4405 (1986).
49 J. Spencer and A. Alavi, Phys. Rev. B **77**, 193110 (2008).
50 R. Sundararaman and T. A. Arias, Phys. Rev. B **87**, 165122 (2013).
51 M. Guidon, J. Hutter, and J. VandeVondele, J. Chem. Theory Comput. **5**, 3010 (2009).
52 F. Hüser, T. Olsen, and K. S. Thygesen, Phys. Rev. B **87**, 235132 (2013).
53 C. Friedrich, S. Blügel, and A. Schindlmayr, Phys. Rev. B **81**, 125102 (2010).
54 T. Kotani and M. van Schilfgaarde, Solid State Comm. **121**, 461 (2002).
55 T. Kotani, M. van Schilfgaarde, and S. V. Faleev, Phys. Rev. B **76**, 165106 (2007).
56 A. Yamasaki and T. Fujiwara, J. Phys. Soc. Jpn. **72**, 607 (2003).
57 M. Gajdoš, K. Hummer, G. Kresse, J. Furthmüller, and F. Bechstedt, Phys. Rev. B **73**, 045112 (2006).
58 M. Shishkin and G. Kresse, Phys. Rev. B **74**, 035101 (2006).
59 J. Yan, J. J. Mortensen, K. W. Jacobsen, and K. S. Thygesen, Phys. Rev. B **83**, 245122 (2011).
60 S. Baroni and R. Resta, Phys. Rev. B **33**, 7017 (1986).
61 J. Hutter, M. Iannuzzi, F. Schiffmann, and J. VandeVondele, WIREs Comput. Mol. Sci. **4**, 15 (2014).
62 The CP2K developers group, CP2K is freely available from: http://www.cp2k.org/ (2017).

[63] O. Vahtras, J. Almlöf, and M. Feyereisen, Chem. Phys. Lett. **213**, 514 (1993).

[64] J. Wilhelm, P. Seewald, M. Del Ben, and J. Hutter, J. Chem. Theory Comput. **12**, 5851 (2016).

[65] P. P. Ewald, Ann. Phys. **369**, 253 (1921).

[66] M. Del Ben, J. Hutter, and J. VandeVondele, J. Chem. Theory Comput. **9**, 2654 (2013).

[67] J. VandeVondele, M. Krack, F. Mohamed, M. Parrinello, T. Chassaing, and J. Hutter, Comput. Phys. Commun. **167**, 103 (2005).

[68] M. Del Ben, O. Schütt, T. Wentz, P. Messmer, J. Hutter, and J. VandeVondele, Comput. Phys. Commun. **187**, 120 (2015).

[69] M. Del Ben, J. Hutter, and J. VandeVondele, J. Chem. Phys. **143**, 102803 (2015).

[70] V. V. Rybkin and J. VandeVondele, J. Chem. Theory Comput. **12**, 2214 (2016).

[71] C. Spreafico and J. VandeVondele, Phys. Chem. Chem. Phys. **16**, 26144 (2014).

[72] J. Cheng and J. VandeVondele, Phys. Rev. Lett. **116**, 086402 (2016).

[73] C. Spreafico and J. VandeVondele, J. Phys. Chem. C **119**, 15009 (2015).

[74] M. Del Ben, J. VandeVondele, and B. Slater, J. Phys. Chem. Lett. **5**, 4122 (2014).

[75] H. N. Rojas, R. W. Godby, and R. J. Needs, Phys. Rev. Lett. **74**, 1827 (1995).

[76] M. M. Rieger, L. Steinbeck, I. White, H. Rojas, and R. Godby, Comput. Phys. Commun. **117**, 211 (1999).

[77] F. Caruso, P. Rinke, X. Ren, A. Rubio, and M. Scheffler, Phys. Rev. B **88**, 075105 (2013).

[78] S.-H. Ke, Phys. Rev. B **84**, 205415 (2011).

[79] T. A. Pham, H.-V. Nguyen, D. Rocca, and G. Galli, Phys. Rev. B **87**, 155148 (2013).

[80] C. Friedrich, M. Betzinger, M. Schlipf, S. Blügel, and A. Schindlmayr, J. Phys. Condens. Matter **24**, 293201 (2012).

[81] G. Lippert, J. Hutter, and M. Parrinello, Mol. Phys. **92**, 477 (1997).

[82] S. Goedecker, M. Teter, and J. Hutter, Phys. Rev. B **54**, 1703 (1996).

[83] M. Krack, Theor. Chem. Acc. **114**, 145 (2005).

[84] J. P. Perdew, K. Burke, and M. Ernzerhof, Phys. Rev. Lett. **77**, 3865 (1996).

[85] J. VandeVondele and J. Hutter, J. Chem. Phys **118**, 4365 (2003).

[86] U. Borštnik, J. VandeVondele, V. Weber, and J. Hutter, Parallel Comput. **40**, 47 (2014).

[87] T. H. Dunning, J. Chem. Phys. **90**, 1007 (1989).

[88] D. E. Woon and T. H. Dunning, J. Chem. Phys. **98**, 1358 (1993).

[89] F. Weigend, A. Köhn, and C. Hättig, J. Chem. Phys. **116**, 3175 (2002).

[90] M. McGrath, J. Siepmann, I.-F. Kuo, and C. Mundy, Mol. Phys. **105**, 1411 (2007).

[91] M. J. McGrath, J. N. Ghogomu, C. J. Mundy, I.-F. W. Kuo, and J. I. Siepmann, Phys. Chem. Chem. Phys. **12**, 7678 (2010).

[92] S. Luber, M. Iannuzzi, and J. Hutter, J. Chem. Phys. **141**, 094503 (2014).

[93] S. Luber, J. Chem. Phys. **141**, 234110 (2014).

[94] P. Partovi-Azar and T. D. Kühne, J. Comput. Chem. **36**, 2188 (2015).

[95] S. Luber, J. Phys. Chem. Lett **7**, 5183 (2016).

[96] M. Guidon, J. Hutter, and J. VandeVondele, J. Chem. Theory Comput. **6**, 2348 (2010).

[97] P. Merlot, R. Izsák, A. Borgoo, T. Kjærgaard, T. Helgaker, and S. Reine, J. Chem. Phys. **141**, 094104 (2014).

[98] J. G. Brandenburg, M. Alessio, B. Civalleri, M. F. Peintinger, T. Bredow, and S. Grimme, J. Phys. Chem. A **117**, 9282 (2013).

[99] J. Klimeš, M. Kaltak, and G. Kresse, Phys. Rev. B **90**, 075125 (2014).

[100] D. Nabok, A. Gulans, and C. Draxl, Phys. Rev. B **94**, 035118 (2016).

[101] P. Liu, M. Kaltak, J. Klimeš, and G. Kresse, Phys. Rev. B **94**, 165109 (2016).

[102] M. J. van Setten, V. A. Popa, G. A. de Wijs, and G. Brocks, Phys. Rev. B **75**, 035204 (2007).

[103] V. G. Plekhanov, V. A. Pustovarov, A. A. O'Konel-Bronin, T. A. Betenekova, and S. O. Cholakh, Sov. Phys. Solid State Phys. **18**, 2438 (1976).